Journal of Molecular Liquids 391 (2023) 123216

Contents lists available at ScienceDirect

Journal of Molecular Liquids

journal homepage: www.elsevier.com/locate/molliq

Thermophysical, rheological and dielectric behaviour of stable carbon black dispersions in PEG200

Marco A. Marcos [a,b,*], Jacek Fal [c], Javier P. Vallejo [d], Gaweł Żyła [c], Luis Lugo [a,*]

[a] CINBIO, Universidade de Vigo, Grupo GAME, Departamento de Física Aplicada, 36310 Vigo, Spain
[b] IDMEC, Instituto Superior Técnico, University of Lisbon, Lisbon 1049-001, Portugal
[c] Department of Physics and Medical Engineering, Rzeszów University of Technology, 35-959 Rzeszów, Poland
[d] Centro Universitario de la Defensa en la Escuela Naval Militar, Grupo InTeam, Plaza de España, s/n, 36920 Marín, Spain

ARTICLE INFO

Keywords:
Polyethylene glycol
Carbon black
Thermal conductivity
Latent heat
Rheological behaviour
Electrical permittivity

ABSTRACT

Phase change materials can store or release large amounts of energy during phase change. An increasing number of authors are studying the influence of the dispersion of nanometric particles on these materials. This article presents the design and experimental characterization of temporal stability, thermal conductivity, isobaric heat capacity, phase change transitions, rheological behaviour, and dielectric properties of nano-enhanced phase change materials based on carbon black (CB) dispersions in polyethylene glycol (PEG200) by using polyvinylpyrrolidone (PVP) as surfactant. We studied the temporal stability of carbon black nanoparticles dispersed in PEG200 using dynamic light scattering and spectrophotometry techniques. All the samples showed good temporal stability, since the measurements of the hydrodynamic size of the nanoparticles are practically constant over time and the wavelength observed by UV–vis shows a small variation of around 4% for static conditions. We observed small changes in thermal conductivity and isobaric heat capacity. Nevertheless, the thermograms evidence how the latent heat clearly increases with the load of carbon black nanoparticles up to four times that of the PEG200. The viscosity studies do not show variation with shear rate, indicating a Newtonian behaviour, excluding the 2.0 wt% CB/PVP + PEG200 nanofluid. Additionally, we noticed frequency dependent and independent regions for permittivity.

1. Introduction

According to the State of Energy and CO_2 Report, there has been a 2.3% global increase in energy consumption over the last decade, which represents almost double the average rate since 2010. This has had an impact on the use of fossil resources, and therefore on global carbon dioxide emissions and the environment [1]. Over recent decades, society has realized that energy efficiency is key to be more respectful with the environment, as well as needing to develop technologies that enable energy to be used appropriately. In order to meet the economic, energetic and environmental challenges, different phase change materials (PCMs) have been proposed for thermal energy storage (TES) systems. Due to the great capacity that PCMs have to release and store thermal energy through phase transitions [2], they have been used in various sectors including heating ventilation and air-conditioning systems [3–5], high-power electronic cooling [6], concentrated solar power systems [7] or food processing [8,9], among other industrial applications.

A TES system must have good storage capacity, fast energy loading and discharge capacity, and is efficient and safe [10]. Additionally, the development of effective energy storage techniques has become a priority for the scientific community in recent decades, as well as improving the performance of energy harvesting techniques where technologies that improve energy systems can help combat climate change while providing energy security [11]. Therefore, TES is considered to be an enabling technology that entails energy management enhancements and stability for both power generation [12–17] and heating and cooling applications [18–21]. Nano-enhanced PCMs (NePCMs) based on low molecular mass poly (ethylene glycol) such as PEG with a molecular mass of 200 $g \cdot mol^{-1}$ (PEG200) can be also used in refrigeration [22,23] owing to their melting points [24,25].

Temporal stability plays a key role in nanofluids, thus many authors are developing nanoparticle dispersions with a surfactant treatment to increase stability. Gallego et al. [26] observed the temporal stability of water-based alumina nanofluids over 5 weeks where sodium dodecyl

* Corresponding authors.
E-mail addresses: mmarcosm@uvigo.es (M.A. Marcos), luis.lugo@uvigo.es (L. Lugo).

https://doi.org/10.1016/j.molliq.2023.123216
Received 31 May 2023; Received in revised form 15 September 2023; Accepted 30 September 2023
Available online 1 October 2023

benzene sulfonate (SDBS) was used as surfactant at 0.32 wt%, obtaining good stability for the dispersion of 0.5 wt% of Al_2O_3wt%. Ordóñez et al. [27] investigated the stability of zirconia nanoparticle dispersions using SDBS, nonionic polyvinylpyrrolidone (PVP), and cationic cetyltrimethylammonium bromide (CTAB) as surfactants. They found that PVP improves the effect on the hydrodynamic diameter further than the other two studied options, and their stability analysis showed a stable 0.01 wt% nanofluid for 20 days. Ma et al. [28] studied the effects on the stability of Al_2O_3-CuO/water and Al_2O_3-TiO_2/water hybrid nanofluids for some surfactants at different temperatures and mass concentrations. They found that the samples containing a small quantity of PVP showed optimum stability even after 25 days with negligible sedimentation.

Organic PCMs have a low capacity to transfer heat by conduction due to their low thermal conductivity but including nanometric particles with high thermal conductivity can improve their thermophysical profile and contribute to increasing and decreasing the speed of fusion and solidification and therefore, performance.

Among other organic phase change materials used as base fluids over recent years, including paraffins, fatty acids, or glycols, PEG is considered a promising material in cold storage due to its stability, recyclability and biodegradability that can be used successfully in organic synthesis [24]. This polymer presents a high latent heat storage and through the molecular mass the melting temperatures can be modified. Recently, several studies have noticed the benefits of this material and it has been used to obtain NePCMs with different types of nanometric particles, such as carbon-based nanoparticles [19,25,29–31] or oxides [31–34], among others.

Current studies in thermal conductivity of different carbon-based nanofluids and NePCMs have attracted attention. Sobczak et al. [35] analysed dispersions of two varieties of carbon black nanopowder with different specific surface areas in ethylene glycol (EG), achieving thermal conductivity improvements of up to 4.8% for the 2% mass concentration of the nanoparticles with the highest surface area. Ilyas et al. [36] studied the dispersion of multi-walled carbon nanotubes with a length of 10–20 μm and a diameter of 30–40 nm in a thermal oil. An enhancement in thermal conductivity up to 28.7% for the 1 wt% concentration was achieved. Colla et al. reported how carbon black nanoparticles enhance the thermal properties of a nanofluid based on paraffin waxes. This study showed a remarkable enhancement of the latent heat of up to 3.4% with respect to base fluid for a dispersion of CB nanoparticles at 1 wt% [37]. Wang et al. obtained an enhancement in the latent heat of a PCM (OP10E), using spherical graphite nanometric particles with a 20 to 30 nm diameter. In this case, the latent heat increases up to 5% for the 2% by weight concentration of graphite in PCM [38]. Lin et al. calculated the heat capacity between 270 and 370 K with a 10 K step for paraffin-based nanocomposites by adding boron nitride. They observed how heat capacity varies with temperature, finding a noticeable peak close to the phase change transition for base fluid and nanofluids. They also reduced latent heat by adding boron nitride nanoparticles to the paraffin [39]. In recent years, many authors have tried to carry out studies on the rheological behaviour of carbon based nanofluids as a function of factors such as the nanoparticle load or temperature [35,40–44]. Aberoumand et al. [45] performed an experimental study for electrochemical nanofluids based on graphene oxide (EGO)/vanadium (IV). They found that the electrolyte-based nanofluids have a Newtonian behaviour for concentrations below 0.05 wt%, but for higher concentrations non-Newtonian behaviour was observed. Ilyas et al. [46] prepared hybrid nanofluids of diamond and graphene nanoplates using a non-ionic stabilizer, showing a noticeable increase of 35% in viscosity for a 2% nanoparticle loading. Finally, some studies on dielectric properties of carbon based nanodispersions have also been performed. Di Rosa et al. [47] studied two different types of nanodiamond powders of 87% and 97% purity in various dispersions between 0.01 and 0.1 wt% in ethylene glycol. They found improvements of electrical conductivity of up to 720% for the purest nanopowders at the highest concentration.

In this work, we designed new stable nano carbon black dispersions in polyethylene glycol by using polyvinylpyrrolidone (PVP) as surfactant with a PVP:CB mass ratio of 1:10. We also performed thorough experimental analyses of temporal stability, thermal conductivity, isobaric heat capacity, phase change transitions, rheological behaviour, and dielectric properties for these nano-enhanced phase change materials.

2. Experimental

2.1. Materials

Dispersions of carbon black, CB, nanopowder in poly(ethylene glycol), PEG200, were designed by using a polyvinylpyrrolidone, PVP, as surfactant (PVP:CB mass ratio of 1:10) to improve the stability of the dispersions. Carbon black nanoparticles were supplied by PlasmaChem (Berlin, Germany). The nanopowder characteristics specified by the manufacturer are shown in Table 1. PEG200 with a mass average molar mass of 259.78 g·mol^{-1} and a polydispersity index of 1.05 [25] was provided by Sigma-Aldrich (Burlington, MA, USA). A polymeric surfactant, polyvinylpyrrolidone, PVP, supplied by BioShop (Burlington, Canada) with an average molar mass of ~40,000 g·mol^{-1} was used.

Table 2 summarises the different NePCMs designed by means of the two-step method, as well as their corresponding PVP + PEG200 base fluids. The studied 0.10, 0.25, 0.50, 0.75, 1.0 and 2.0% carbon black nanoparticle concentrations with 1:10 PVP:CB mass ratio were first mechanically mixed for 30 min with an IKA Genius 3 Vortex (Staufen, Germany). These dispersions were then sonicated for 200 min in an EMAG Emmi 60 HC (Moerfelden-Walldorf, Germany) ultrasonic bath, in which water was continuously recirculated to ensure stable sample temperature. Lastly, all samples were further sonicated for 3 min by a Sonics Vibracell VCX130 (Newtown, USA) high-energy ultrasonic probe working at 50% amplitude with a step program of 10 s ON out of each 30 s.

2.2. Nanopowder characterization

The morphology of the carbon black nanoparticles was examined by scanning electron microscopy (SEM) by using a JEOL JSM-6700F SEM microscope (Tokyo, Japan), and by transmission electron microscopy (TEM) through a JEM-2010F TEM microscope (Tokyo, Japan). Moreover, the chemical composition of the carbon black nanopowder was assessed by energy dispersive X-ray spectroscopy (EDS) microanalysis using an Oxford Instruments-Inca Energy 300 spectrometer (Oxford, UK) attached to the SEM microscope. The study was carried out on silica supports (SEM, EDS) and copper supports (TEM). Some drops of nanoparticles dispersed in methanol were placed on each support and dried at room temperature. Fig. 1 contains SEM and TEM images of the carbon black nanopowder used, showing the regular shape of the carbon black nanoparticles. The nanoparticle size declared by the manufacturer, ~13 nm in diameter, can be confirmed according to the images. Fig. 2 shows

Table 1
Manufacturer specifications for commercial carbon black nanopowder.

Nanoadditive	Carbon black
Manufacturer	PlasmaChem
Composition	Mesoporous carbon, C ≤ 100%
CAS No.	7782–40-3
Appearance	Form: powder, Colour: black
Relative density	1,500–1,900 g·cm^{-3}
Auto-ignition temperature	> 588.15 K
Average particle size	ca. 13 nm
Specific surface area	ca. 570 ± 20 m^2·g^{-1}
Purity	> 99%
Other contents	Ash < 0.02%

Table 2
List of designed samples.

Nanofluid	Base fluid	PVP:CB mass ratio	PVP:PEG200 mass ratio
0.01 wt% CB/PVP + PEG200	0.001 wt% PVP + PEG200	1:10	1:100000
0.10 wt% CB/PVP + PEG200	0.010 wt% PVP + PEG200	1:10	1:10000
0.25 wt% CB/PVP + PEG200	0.025 wt% PVP + PEG200	1:10	1:4000
0.50 wt% CB/PVP + PEG200	0.050 wt% PVP + PEG200	1:10	1:2000
0.75 wt% CB/PVP + PEG200	0.075 wt% PVP + PEG200	1:10	1:1333
1.0 wt% CB/PVP + PEG200	0.10 wt% PVP + PEG200	1:10	1:1000
2.0 wt% CB/PVP + PEG200	0.20 wt% PVP + PEG200	1:10	1:500

the EDS microanalysis of the carbon black nanoparticles. The results report a larger presence of carbon (C), as expected, and the emergence of oxygen (O) in a lower percentage. The silica (Si) peak is obtained due to the used support. In a previous study [35], the Brunauer-Emmett-Teller (BET) specific surface area of the nanoadditive was experimentally determined by nitrogen physisorption. The reported BET surface area was 450 ± 8 $m^2 \cdot g^{-1}$.

2.3. Methods

The hydrodynamic diameter of the PVP-supported CB nanoparticle dispersions in PEG200 over time was analysed by using a Marvern Zetasizer Nano ZS (Malvern, UK). The operating principle of this device is based on the dynamic light scattering (DLS) technique, which provides the hydrodynamic diameter of the carbon black nanoparticles in dispersion from the measurement of the translational diffusion coefficient that characterises Brownian movement and is described in the ISO standard ISO 22412:2017 [48]. A scattering angle of 173° and a temperature of 293 K were selected as operating parameters. The average standard deviation of the size measurements was declared lower than 3.5%. A Cary 5000 UV–Vis–NIR spectrophotometer from Agilent (Santa Clara, USA) was used to determine the absorbance in the range of wavelength 210–710 nm at room temperature.

Thermal conductivity, *k*, was evaluated from 283.15 to 333.15 K by using a Decagon KD2 Pro Thermal Analyzer (Pullman, USA), based on transient hot wire (THW) technique [49,50]. This equipment was equipped with a KS-1 sensor with a length of 60 mm and diameter 1.27 mm that, vertically inserted into the middle of the samples, is appropriated and performs the thermal conductivity measurements of the fluids. Distilled water was used as calibration liquid and an expanded uncertainty in the thermal conductivity measurement was less than 3% for temperatures ranging from 293.15 to 323.15 K [51,52].

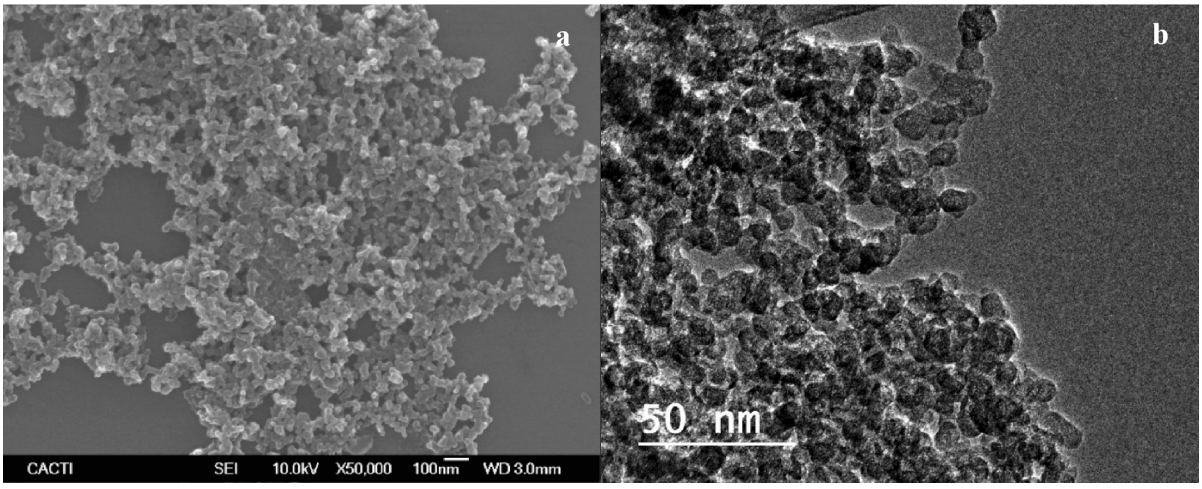

Fig. 1. Scanning electron microscopy image (a) and transmission electron microscopy image (b) of the carbon black nanopowder.

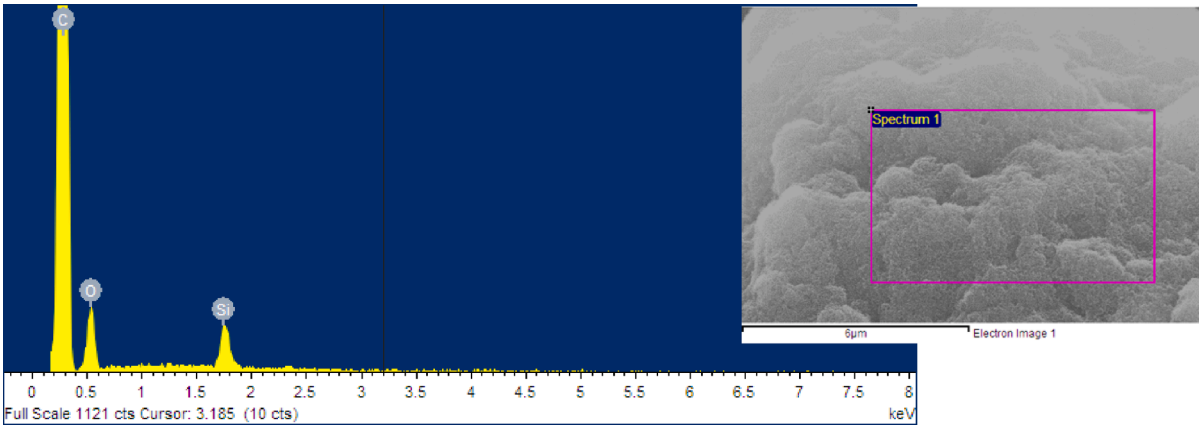

Fig. 2. Energy-dispersive X-ray spectroscopy microanalysis of the carbon black nanopowder.

Phase change melting temperatures were obtained using a heat flow type differential scanning calorimeter TA Instruments DSC Q2000 (New Castle, DE, USA). We determined them using a heating rate of 2 K/min. Nitrogen with a flow rate of 50 ml·min^{-1} and a purity in terms of mole fraction $\geq$ 0.99999 was used to maintain an inert atmosphere and to cool the designed dispersions and base fluids during the freezing process with a refrigerated cooling system RSC90. Each measurement was repeated 3 times to confirm reproducibility. This device gives estimated enthalpies and temperatures where the expanded uncertainties are 0.3 K and 1.2 J·g^{-1}, respectively [53].

Isobaric heat capacities, c_p, were analysed by the previously described DSC Q2000 calorimeter, which worked under the quasi-isothermal temperature modulated differential scanning calorimetry method (TMDSC). The temperature applied to the samples was modulated with a period of 80 s and an amplitude of 0.5 K for 30 min. The temperature range studied was between 233.15 and 353.15 K where the expanded uncertainty of the experimental c_p is 3% [53].

The rheological behaviour was analysed by a Thermo Electron HAAKE MARS 2 rheometer (Karlsruhe, Germany) at 298.15 K. A cone-plate geometry (Haake C60) with 60 mm diameter, 0.106 mm gap, and 2° cone angle was used. The rheometer is also equipped with a Peltier system with a HAAKE C25P refrigerated bath with a Phoenix II controller. This system ensures the set temperature with 0.1 K accuracy. A shear rate range from 10 to 1000 s^{-1} was used to measure the flow curves. Dynamic viscosities, μ, were considered as the average value in the shear rate range from 10 to 1000 s^{-1}. The reported values achieved the comparability, repeatability, and reproducibility requirements of the ASTM D445 standard. The expanded uncertainty of the μ measurements was 5% [54,55].

Electrical permittivity was evaluated using a Novocontrol Technologies Concept 80 (Montabaur, Germany) broadband dielectric spectroscopy system. The measuring stand measures a wide range of frequencies and temperatures. The frequency was changed from 10 MHz to 1 Hz in 67 steps using a logarithmic scale. The samples were placed in a Novocontrol Technologies KG BDS 1309 (Montabaur, Germany) measuring cell with 11 mm in diameter and 5.5 mm in height. The temperature was stabilised at 293.15 K with an accuracy of 0.5 K at least 15 min before the measurements. For this purpose, the Novocontrol Technologies KG Quatro Cryosystem (Montabaur, Germany) was working as a heating/cooling system. An ohmic standard calibration was developed prior to the measurements following the manufacturer's recommendations [56].

3. Results

3.1. Temporal stability

The low concentrated 0.10 wt% CB/PVP + PEG200 nanofluid was examined for stability analysis. Fig. 3 shows the temporal evolution of the Z-average size of CB nanoparticles dispersed in PEG200 with PVP used as surfactant. One of the dispersions was subjected to mechanical agitation using a vortex mixer (shaken sample) and the other remained in stationary conditions during the whole study (static sample). The Z-average size for the two samples remained constant over time, which confirmed the stability of the dispersions. There was no sedimentation or agglomeration of the nanoparticles for 4 weeks. Furthermore, no significant differences were detected between static and shaken samples, since the mean hydrodynamic size during the study period was 127 and 130 nm, respectively. Therefore, it can be confirmed that the designed dispersions show a long-term stability (static sample) and have a good dispersibility (shaken sample).

The hydrodynamic size distribution by intensity of the 0.10 wt% CB/PVP + PEG200 nanofluid was measured by DLS. Thus, the size distribution for the static and shaken samples was compared after preparation with 28 days later. The results are shown in Fig. 4, where it can be verified that the size distribution does not significantly vary.

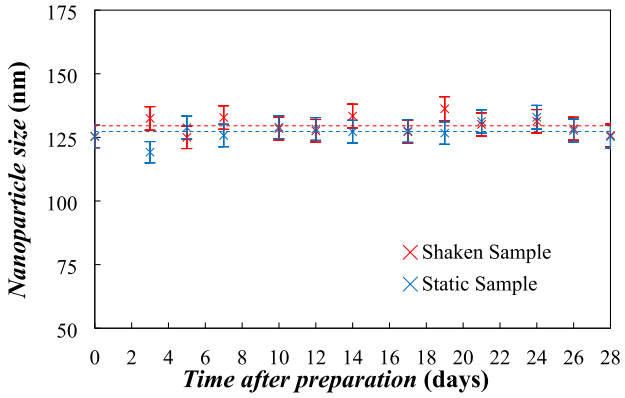

Fig. 3. Temporal evolution of nanoparticle Z-average size for the 0.10 wt% CB/PVP + PEG200 nanofluid under static and shaken conditions. Error bars correspond to expanded size uncertainty (k = 2) and dashed lines to average value.

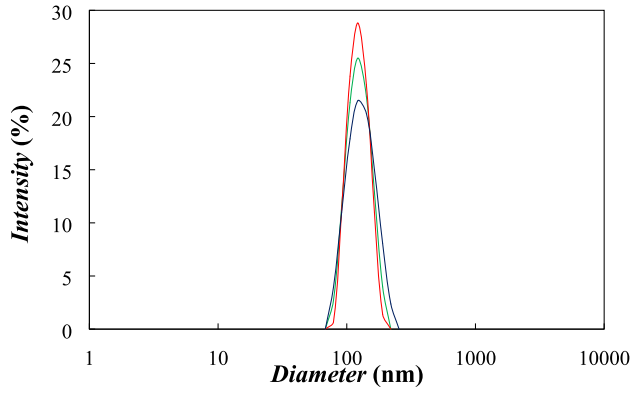

Fig. 4. Hydrodynamic size distribution by intensity for the 0.10 wt% CB/PVP + PEG200 nanofluid just after preparation (—), and 28 days later for static sample (—) and shaken sample (—).

The absorption spectrum for the most diluted nanofluid was analysed i.e., 0.01 wt% CB/PVP + PEG200. Fig. 5 shows the absorbance curve for this dispersion, and the maximum value of the curve was close to 250 nm.

To confirm the good stability results of the new NePCM, a 250 nm wavelength was selected, where the evolution of the absorbance over the time was analysed. Thus, the stability of the value was scrutinised for 300 h, taking the measurements every 10 min. Fig. 6a shows the

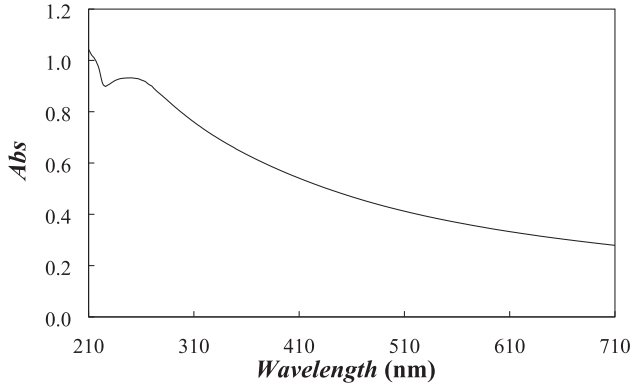

Fig. 5. Optical absorption spectra for the most diluted nanofluid, 0.01 wt% CB/PVP + PEG200, after preparation at 298.15 K.

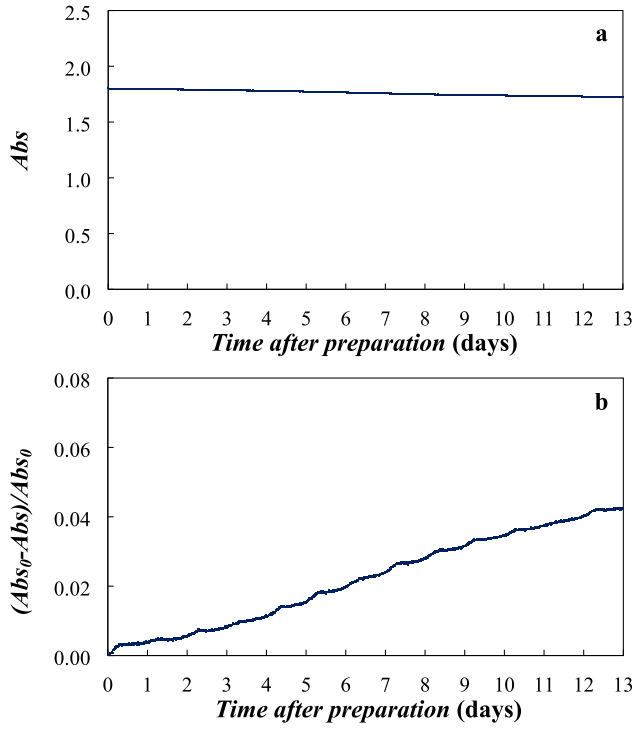

Fig. 6. (a) Kinetic deposition and **(b)** percent decrease of absorbance for the 0.01 wt% CB/PVP + PEG200 nanofluid at 250 nm wavelength and 298.15 K.

absorbance evolution during this period. The kinetic deposition at the selected wavelength showed slight variations demonstrating a stable sample.

Furthermore, Fig. 6b shows the temporal evolution of the absorbance variation during the period studied, where we registered decreases in absorbance of 1.2%, 3.0% 4.2% after 4, 8 and 12 days, respectively.

3.2. Thermal conductivity

The experimental values obtained for PEG200 agree with the data garnered by Gómez–Merino [57], Dubyk et al. [58], Sun et al. [59], and Rebrović et al. [60], with deviations between 1.9% and 8.8%. These comparisons were made at 298.15 K, although the isotherms and molecular mass for some literature data are not always reported for the said PEG200 samples. The influence of the temperature on thermal conductivity was analysed for PEG200, but also for all base fluids and nanofluids, and similar decreases with increasing temperature were found. As an example, Fig. 7a shows these temperature dependences for PEG200, the highest concentrated nanofluid (2.0 wt% CB/PVP + PEG200) and its corresponding base fluid (0.20 wt% PVP + PEG200), ~2.5 %. These decreases were found in the analysed temperature range for all samples. In addition, no thermal conductivity enhancement for the highest CB loaded sample was proven, as the differences were lower than the accuracy of the experimental method. Spahr et al. [61] states that, compared to other graphite powders, carbon black nanomaterials exhibit significantly lower thermal conductivities ranging from 0.1 to 0.5 W m^{-1} K^{-1}. Thus, although other carbon nanoparticles such as carbon nanotubes and nanofibers [62–64], or graphene nanoplatelets [65,66], have significantly enhanced the thermal conductivity of many types of PCM, the improvements provided by carbon black nanoadditives are smaller. These slight increases have also been observed in the literature for other CB nanofluids based on ethylene glycol. Sobczak et al. [35] studied the experimental values of the thermal conductivity of CB-EG nanofluids at 298.15 K using two types of carbon black nanoparticles with different specific surface area (SSA). Their results showed that CB nanoparticles with a SSA of ~570 $m^2 \cdot g^{-1}$ (the same as in this work, see Section 2.2) reached a maximum increase of 1.2% for the 2 wt % nanoadditive concentration. However, nanoparticles with a larger SSA, ~1000 $m^2 \cdot g^{-1}$, reached increases of up to 4.8% for the same nanoparticle loading.

The effect of the addition of PVP to PEG200 on thermal conductivity is nearly insignificant in the PVP concentration range of Table 2 (up to 0.20 wt% PVP), although it seems that PVP produce a benefit in terms of this transport property. To analyse the hypothetical effect of PVP, thermal conductivity of PVP + PEG200 samples at PVP concentrations higher than those mentioned in Table 2 were considered. Fig. 7b shows maximum increases of around 1.6% even for 5.0 wt% PVP concentration. Similar effects were also observed when adding PVP to deionized water, as reported by Mingzheng et al. [67]. Consequently, considering the worsening effect in terms of viscosity by using superior PVP concentrations in the base fluids, the selected PVP ratio was reasserted.

3.3. Differential scanning calorimetry

Fig. 8 shows the solid–liquid phase transitions for the base fluids, PEG200, the 0.20 wt% PVP + PEG200 base fluid, and the different CB/PVP + PEG200 nanofluids at 2 K·min^{-1} heating rate. To validate the results, the samples were studied under three cyclical repetitions.

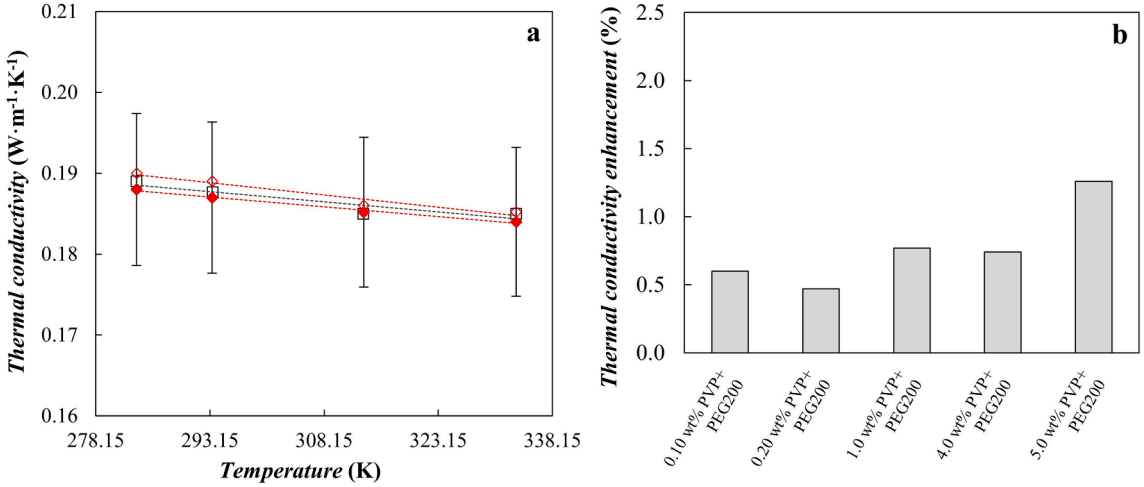

Fig. 7. (a) Temperature dependence of thermal conductivity for PEG200 (□), 0.20 wt% PVP + PEG200 base fluid (◇), and 2.0 wt% CB/PVP + PEG200 nanofluid (◆). Error bars correspond to expanded thermal conductivity uncertainty (k = 2). **(b)** Thermal conductivity enhancements for different PVP + PEG200 samples.

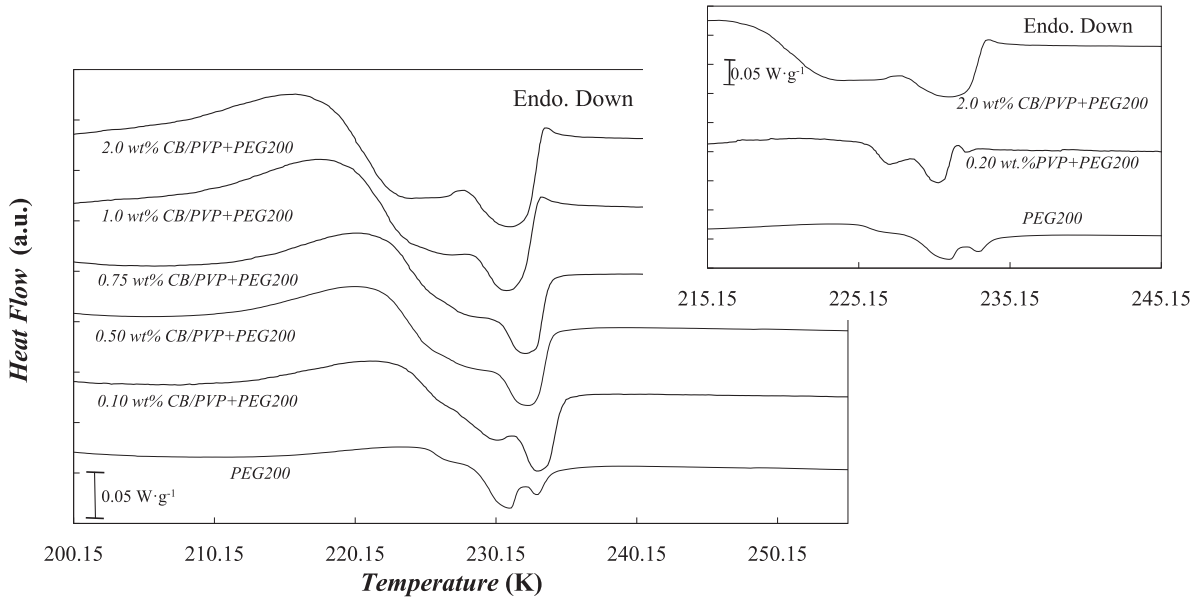

Fig. 8. DSC heating thermograms at 2 K·min^{-1} heating rate for PEG200 and different CB/PVP + PEG200 nanofluids. Inset: Results for PEG200, 0.20 wt% PVP + PEG200 base fluid, and 2.0 wt% CB/PVP + PEG200 nanofluid.

It is observed that the dispersion of carbon black in PEG200 has a huge impact on the latent heat and involves a small shift of the curves. Three endothermic peaks are observed for PEG200 reaching their maximum values at 233, 231 and 226 K that may be explained by the degree of polydispersity of PEG200. A smoothing of these peaks is observed as the concentration of CB is increased, and two peaks are shown for the highest CB concentrations. With the aim to elucidate the distinctive effect of PVP and CB nanoparticles on the transition of PEG200 the inset of Fig. 8 and Table 3 also include those results for the 0.20 wt% PVP + PEG200 base fluid. The ratio of this mixture is that corresponding to the base fluid of the highest loaded nanofluid. As observed, the addition of PVP surfactant maintains the phase change characteristics of PEG200 preserving the three endothermic peaks. However, the dispersion of CB nanoparticles entails a slight shift of the curve to the left which means a valuable maximum reduction of 2.2 K of subcooling. The latent heat of fusion reaches a maximum value of 32.2 J·g^{-1} for the 2.0 wt% CB/PVP + PEG200 nanofluid which involves increases of the order of four times the PEG200 sample and/or the 0.20 wt % PVP + PEG200 base fluid.

The isobaric heat capacities were measured for PEG200, the highest concentrations in CB nanoparticles and their corresponding base fluids to show the influence of both surfactant and nanoadditive. The experiments were performed over a wide temperature range and far enough away from the phase transition to avoid inaccurate measurements. The c_p temperature dependences can be observed in Fig. 9 and rises around 13% for all samples within the depicted temperature interval are found. These temperature dependences agree with those reported in the literature for other polyethylene glycols, PEG200 [68] and PEG400 [65,68].

Adding PVP to PEG200 entails an average isobaric heat capacity decrease of 3% and 6% for the 0.10 wt% and 0.20 wt% PVP + PEG200 base fluids, respectively. Similarly, the isobaric heat capacity decreases with the solid nanoparticle loading with average reductions of 1.5% and 3.2% for the 1.0 wt% and 2.0 wt% CB/PVP + PEG200 nanofluids over the mentioned based fluids, respectively. Similar effects due to nanoadditive dispersions were observed for different carbon-based nanoparticles [63,65,69]. Thus, previous literature works report isobaric heat capacity decreases of 3% for fullerenol $C_{60}(OH)_{22\text{-}24}$ dispersed in water [69], 0.34% for graphene nanoplatelets (0.5 wt%) [65] and 3% for multi-walled carbon nanotubes (1 wt%) dispersed in PEG400 [63] with similar molecular mass, 400 g·mol^{-1}.

3.4. Rheological behaviour

To properly analyse the individual effect of the dispersed CB nanoparticles on the rheological behaviour, it is necessary to compare each dispersion with its corresponding PVP + PEG200 base fluid. The flow curves shown in Fig. 10 evidence Newtonian behaviours for PEG200 and all base fluids, at 298.15 K as an example. The here reported viscosity for PEG200 at 298.15 K, 50.1 mPa·s, agrees well with the obtained values from the available literature [25,70–73]. Deviations of 4.1%, 0.8%, −5.5%, −0.5%, and 0.8% were observed with values from Ottani et al. [70], Vuksanović et al. [71], Marcos et al. [25], Wu et al. [72], and

Table 3
Latent heat, L_h, and melting point, T_m, for PEG200, 0.20 wt% PVP + PEG200 base fluid, and different CB nanofluids at 1 K·min^{-1} heating rate. Latent heat enhancements are referred to PEG200.

Sample	L_h (J·g^{-1})	T_m (K)	$(L_{h\ sample} - L_{h\ PEG200})/ L_{h\ PEG200}) \times 100$
PEG200	7.2	233.0	–
0.20 wt% PVP + PEG200*	8.1	232.0	12%
0.10 wt% CB/PVP + PEG200	16.1	233.0	123%
0.50 wt% CB/PVP + PEG200	18.9	232.1	162%
0.75 wt% CB/PVP + PEG200	20.5	232.1	184%
1.0 wt% CB/PVP + PEG200	24.7	230.7	241%
2.0 wt% CB/PVP + PEG200	32.2	230.8	345%

*Base fluid corresponding to the 2.0 wt% CB nanofluid.

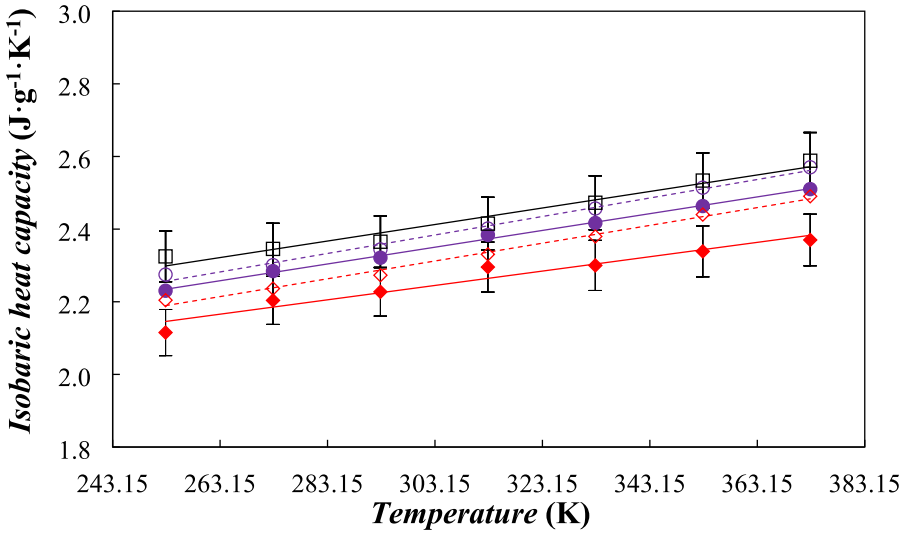

Fig. 9. Isobaric heat capacities for PEG200 (□), the PVP + PEG200 base fluids with PVP concentrations: 0.10 wt% (○) and 0.20 wt% (◇), and the CB/PVP + PEG200 nanofluids with CB nanoparticle loadings: 1.0 wt% (●) and 2.0 wt% (◆). Error bars correspond to c_p expanded uncertainty (k = 2).

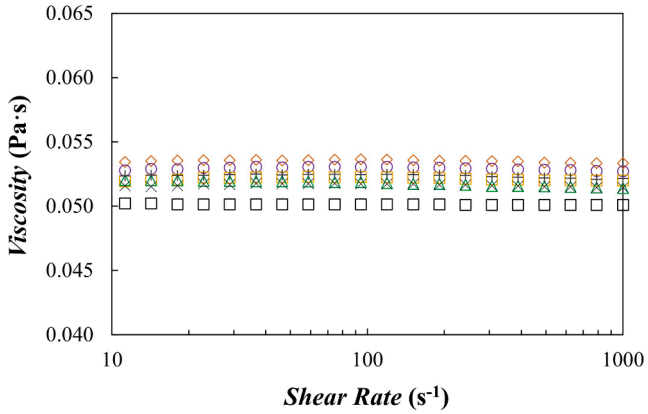

Fig. 10. Flow curves for PEG200 (□) and PVP + PEG200 base fluids at 298.15 K. PVP concentrations: 0.010 wt% (△), 0.025 wt% (×), 0.050 wt% (□), 0.075 wt% (+), 0.10 wt% (○), and 0.20 wt% (◇).

Živković et al. [73], respectively. The explored PVP concentrations entail viscosity rises of up to 6.7% in relation to PEG200. A similar behaviour in viscosity was found by Zhang et al. [74] for aqueous PVP solutions.

Similarly, Newtonian behaviour is found for all nanofluids except 2.0 wt% CB/PVP + PEG200, as observed in Fig. 11a at 298.15 K, for example. Likewise, Yapici et al. [34] reported that the dispersion of titanium oxide nanoparticles in PEG200 entails a pseudoplastic behaviour at low shear rates for concentrations between 1 and 2% wt%. Viscosity rises regarding PEG200 for the Newtonian nanofluids reach 8.6%, as observed in this figure. As reported in the literature, CB dispersions in different base fluids involve low viscosity worsening in comparison with other carbon based nanoadditives like nanodiamonds, graphite/diamond mixtures, graphene nanoplatelets, or multi-walled carbon nanotubes [25,42,63]. Thus, viscosity increases of 13% were reported for a 0.50 wt% CB dispersion in ethylene glycol:water mixture 50:50 vol% while increases reached 27% for a 0.50 wt% nanodiamond dispersion in the same base fluid [42]. Likewise, increases up to 102% were reported for dispersions of multi-walled carbon nanotubes in PEG200 at nanoadditive concentrations of up to 0.7 wt% [25]. These rises reach 71% and 30% for multi-walled carbon nanotubes dispersions in PEG300 and PEG400, respectively [25,63].

On the other hand, Fig. 11b shows the percentual viscosity rises for the Newtonian nanofluids regarding each PEG + PVP base fluid, and their maximum increments were 3.2%. Therefore, the dispersion of CB nanoparticles means a lower contribution to the viscosity increases of nanofuids than that of the addition of PVP surfactant.

3.5. Electrical permittivity

Fig. 12a presents the real part of the complex permittivity (ε') of PEG200 with various PVP contents as a function of frequency at 293.15 K. The obtained data can be divided into two regions. Below 2 kHz, the increasing frequency causes a noticeable decrease in ε', in accordance with the literature [75]. High changes in this frequency band may be caused by two factors. The first is the effect of electrode polarization [76,77], while the second is due to Maxwell-Wagner polarization [77]. It is also observed that the addition of PVP to PEG200 causes an electrical permittivity reduction in this low frequency range. Above the 2 kHz, ε' is not affected by the frequency changes for PEG200 and PVP + PEG base fluids, while permittivity increases of around 55 % are reached due to adding PVP. Similarly, frequency dependent and independent regions were observed by Saraswat and Sengwafor [78] for ZnO dispersions in a mixture of ethylene glycol and glycerol, where a frequency crossover point occurs also around 1 kHz.

Fig. 12b shows the real part of the complex permittivity as a function of frequency for PEG200 and different CB/PVP + PEG200 nanofluids at 293.15 K. As can be observed, the presence of both dependent and non-dependent frequency regions is maintained for nanofluids, and a similar above-mentioned frequency crossing point is exhibited. The permittivity increases for nanofluids rise with concentration at high frequencies and these enhancements are very similar to those corresponding to PVP + PEG200 base fluids. Therefore, PVP entails the main influence in permittivity values of the samples in this non-dependent frequency region. Likewise, carbon black nanoparticles lead to a reduction of permittivity data at low frequencies like the contribution of PVP.

4. Conclusions

In this study, we designed new carbon black-enhanced phase change materials, CB/PVP + PEG200. The load of CB nanoparticles in PEG200 has been studied from 0.10 wt% to 2.0 wt%, with a PVP:CB mass ratio of 1:10.

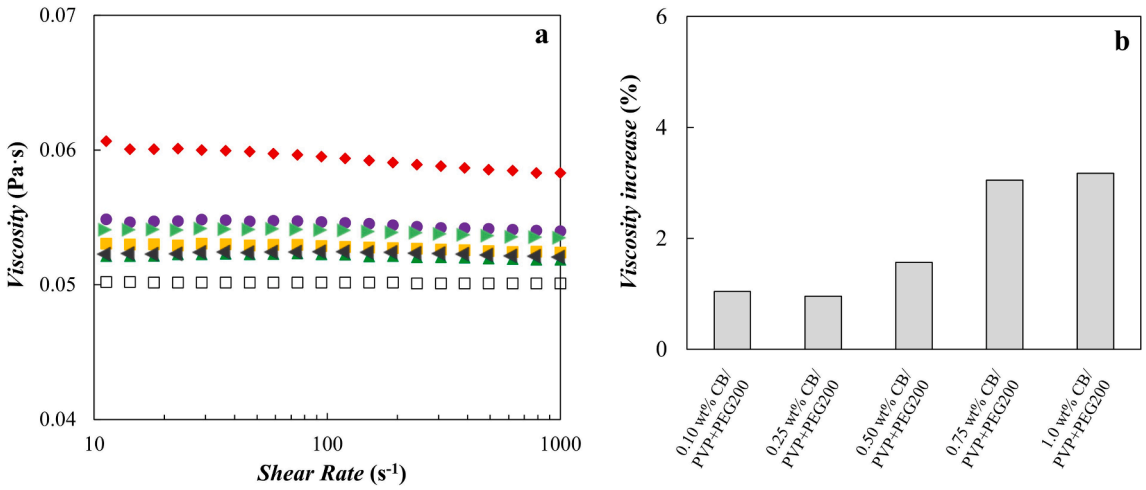

Fig. 11. **(a)** Viscosity for PEG200 (□) and CB/PVP + PEG200 nanofluids at 298.15 K. CB nanoparticle loadings: 0.10 wt% (▲), 0.25 wt% (◀), 0.50 wt% (■), 0.75 wt % (▶), 1.0 wt% (●), and 2.0 wt% (◆). **(b)** Viscosity increases of Newtonian nanofluids with respect to each base fluid at 298.15 K.

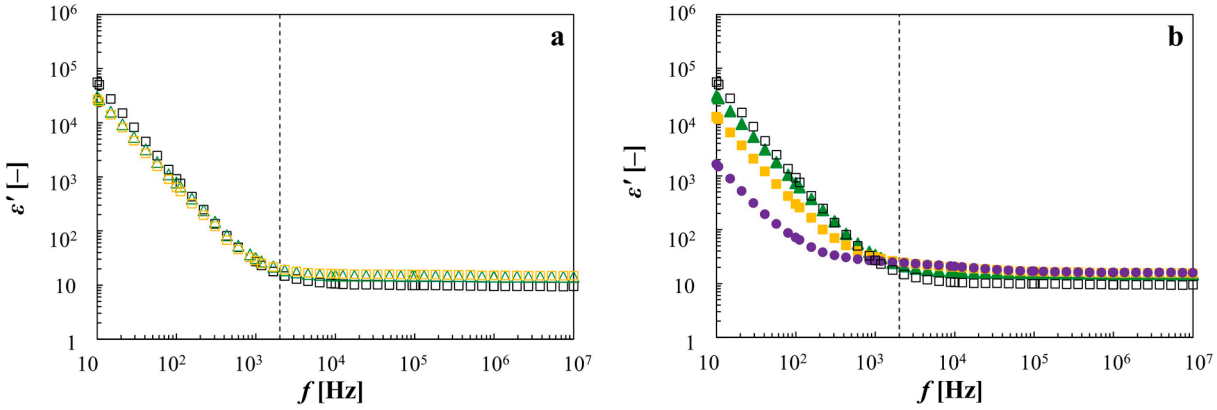

Fig. 12. Real part of complex permittivity against frequency at 293.15 K for **(a)** PEG200 (□), PVP + PEG200 base fluids with PVP concentrations: 0.010 wt% (△) and 0.050 wt% (□), and **(b)** CB/PVP + PEG200 nanofluids with CB nanoparticle loadings: 0.10 wt% (▲), 0.50 wt% (■), and 1.0 wt% (●).

- The experimental characterization of their temporal stability, thermal conductivity, solid–liquid phase transitions, isobaric heat capacity, rheological behaviour, and electrical permittivity were found.
- The addition of PVP surfactant increases the stability of the dispersions, obtaining stable samples according to DLS and UV–vis measurements. The Z-average size for both static and shaken samples remain constant and we observed slight decreases in absorbance.
- There was no thermal conductivity enhancement for CB nanofluids and the effect of the addition of PVP to PEG200 is nearly insignificant.
- The dispersion of CB nanoparticles entails a remarkable increment of the latent heat of fusion and a slight shift of the melting curves to the left which means a valuable maximum reduction of 2.2 K of subcooling. The latent heat of fusion increases up to four times with respect to that of PEG200 and/or the 0.20 wt% PVP + PEG200 base fluid.
- The PVP surfactant addition to PEG200 entails isobaric heat capacity decreases of up to 6% while the dispersion of CB nanoparticles to PVP + PEG200 base fluids leads to heat capacity reductions up to 3.2%.
- We found Newtonian behaviour in all samples, except for the 2.0 wt % CB/PVP + PEG200 nanofluid. The addition of PVP surfactant leads to the highest contribution to the viscosity increases for the Newtonian nanofluids. We also observed increases of up to 8.6% regarding PEG200 and up to 3.2% regarding the PEG + PVP base fluids.
- The impact of CB nanoparticles and PVP surfactant on the electrical permittivity of PEG200 shows frequency dependent and independent regions. We noted noticeable increases in the electrical permittivity for the most concentrated nanofluids at high frequencies, mainly due to PVP addition.

CRediT authorship contribution statement

Marco A. Marcos: Conceptualization, Methodology, Investigation, Formal analysis, Writing – original draft, Writing – review & editing. **Jacek Fal:** Investigation, Formal analysis, Data curation, Writing – original draft. **Javier P. Vallejo:** Conceptualization, Methodology, Investigation, Writing – review & editing. **Gaweł Żyła:** Conceptualization, Methodology, Writing – review & editing, Supervision. **Luis Lugo:** Project administration, Conceptualization, Resources, Writing – review & editing, Supervision.

Declaration of Competing Interest

The authors declare that they have no known competing financial interests or personal relationships that could have appeared to influence the work reported in this paper.

Data availability

Data will be made available on request.

Acknowledgements

Grant PID2020-112846RB-C21 funded by MCIN/AEI/10.13039/501100011033. Grant PDC2021-121225-C21 funded by MCIN/AEI/10.13039/501100011033 and by "European Union NextGenerationEU/PRTR". This work was partially supported by the EU COST Innovators Grant CIG15119: Nanofluids for Convective Heat Transfer Devices, NANOConVEX and M.A.M. acknowledges EU COST for the STMS grants ref. COST-STSM-CA15119-45123 and the financial support by the Ministerio de Universidades (Spain) under budgetary implementation 33.50.460A.752 and by the European Union NextGenerationEU/PRTR through a Margarita Salas postdoctoral contract of the Universidade de Vigo (Spain). J.P.V. thanks the Defense University Center at the Spanish Naval Academy (CUD-ENM) for all the support provided for this research.

References

[1] G.E. Iea, CO_2 Status Report 2018, International Energy Agency, Paris, France, 2019.
[2] H. Mehling, L.F. Cabeza, Heat and cold storage with PCM, Springer, 2008.
[3] P. McKenna, W.J. Turner, D. Finn, Geocooling with integrated PCM thermal energy storage in a commercial building, Energy 144 (2018) 865.
[4] S. Ručevskis, P. Akishin, A. Korjakins, Parametric analysis and design optimisation of PCM thermal energy storage system for space cooling of buildings, Energ. Build. 224 (2020), 110288.
[5] G. Alva, Y. Lin, G. Fang, An overview of thermal energy storage systems, Energy 144 (2018) 341.
[6] S. Motahar, R. Khodabandeh, Experimental study on the melting and solidification of a phase change material enhanced by heat pipe, Int. Commun. Heat Mass Transf. 73 (2016) 1.
[7] Y. Li, Z. Ding, M. Shakerin, N. Zhang, A multi-objective optimal design method for thermal energy storage systems with PCM: A case study for outdoor swimming pool heating application, J. Energy Storage 29 (2020), 101371.
[8] M. Alomair, Y. Alomair, S. Tasnim, S. Mahmud, H. Abdullah, Analyses of Bio-Based Nano-PCM filled Concentric Cylindrical Energy Storage System in Vertical Orientation, J. Energy Storage 20 (2018) 380.
[9] P.M. Kumar, R. Elakkiyadasan, N. Sathishkumar, G.A. Prabhu, T. Balasubramanian, Performance enhancement of a domestic refrigerator with Nanoparticle Enhanced PCM over the condenser side, FME Trans. 48 (2020) 620.
[10] A. Sharma, S.K. Kar, Energy sustainability through green energy, Springer, 2015.
[11] M.C. Lott, S. Kim, C. Tam, D. Houssin, J. Gagné, Technology roadmap: energy storage, Paris, France, International Energy Agency, 2014.
[12] A. Alashkar, M. Gadalla, Thermo-economic analysis of an integrated solar power generation system using nanofluids, Appl. Energy 191 (2017) 469.
[13] Z. Bai, Q. Liu, J. Lei, X. Wang, J. Sun, H. Jin, Thermodynamic evaluation of a novel solar-biomass hybrid power generation system, Energy Convers. Manag. 142 (2017) 296.
[14] Z. Ding, H. Hou, G. Yu, E. Hu, L. Duan, J. Zhao, Performance analysis of a wind-solar hybrid power generation system, Energy Convers. Manag. 181 (2019) 223.
[15] E. González-Roubaud, D. Pérez-Osorio, C. Prieto, Review of commercial thermal energy storage in concentrated solar power plants: Steam vs. molten salts, Renew, Sustain. Energy Rev. 80 (2017) 133.
[16] U. Pelay, L. Luo, Y. Fan, D. Stitou, M. Rood, Thermal energy storage systems for concentrated solar power plants, Renew. Sustain. Energy Rev. 79 (2017) 82.
[17] M.T. White, A.I. Sayma, A new method to identify the optimal temperature of latent-heat thermal-energy storage systems for power generation from waste heat, Int. J. Heat Mass Transf. 149 (2020), 119111.
[18] M. Aqib, A. Hussain, H.M. Ali, A. Naseer, F. Jamil, Experimental case studies of the effect of Al_2O_3 and MWCNTs nanoparticles on heating and cooling of PCM, Case Stud. Therm. Eng. 22 (2020), 100753.
[19] D. Cabaleiro, S. Hamze, J. Fal, M.A. Marcos, P. Estellé, G. Żyła, Thermal and physical characterization of PEG phase change materials enhanced by carbon-based nanoparticles, Nanomaterials 10 (2020) 1168.
[20] M.A. Marcos, D. Cabaleiro, S. Hamze, L. Fedele, S. Bobbo, P. Estellé, L. Lugo, NePCM based on silver dispersions in poly(ethylene glycol) as a stable solution for thermal storage, Nanomaterials 10 (2020) 19.
[21] S. Valizadeh, M. Ehsani, M. Torabi Angji, Development and thermal performance of wood-HPDE-PCM nanocapsule floor for passive cooling in building, Energy Sources Part A Recovery Util, Environ. Eff. 41 (2019) 2114.
[22] M. Liu, W. Saman, F. Bruno, Development of a novel refrigeration system for refrigerated trucks incorporating phase change material, Appl. Energy 92 (2012) 336.
[23] W. Lu, S. Tassou, Characterization and experimental investigation of phase change materials for chilled food refrigerated cabinet applications, Appl. Energy 112 (2013) 1376.
[24] A.A. Minea, State of the art in PEG-based heat transfer fluids and their suspensions with nanoparticles, Nanomaterials 11 (2021) 86.
[25] M.A. Marcos, L. Lugo, S.V. Ageev, N.E. Podolsky, D. Cabaleiro, V.N. Postnov, K. N. Semenov, Influence of molecular mass of PEG on rheological behaviour of MWCNT-based nanofluids for thermal energy storage, J. Mol. Liq. 318 (2020), 113965.
[26] A. Gallego, K. Cacua, B. Herrera, D. Cabaleiro, M.M. Piñeiro, L. Lugo, Experimental evaluation of the effect in the stability and thermophysical properties of water-Al_2O_3 based nanofluids using SDBS as dispersant agent, Adv. Powder Technol. 31 (2020) 560.
[27] F. Ordóñez, F. Chejne, E. Pabón, K. Cacua, Synthesis of ZrO_2 nanoparticles and effect of surfactant on dispersion and stability, Ceram. Int. 46 (2020) 11970.
[28] M. Ma, Y. Zhai, P. Yao, Y. Li, H. Wang, Effect of surfactant on the rheological behavior and thermophysical properties of hybrid nanofluids, Powder Technol. 379 (2021) 373.
[29] T. Qian, J. Li, W. Feng, H.e., Nian, Single-walled carbon nanotube for shape stabilization and enhanced phase change heat transfer of polyethylene glycol phase change material, Energy Convers, Manag. 143 (2017) 96.
[30] R. Singh, S. Sadeghi, B. Shabani, Thermal conductivity enhancement of phase change materials for low-temperature thermal energy storage applications, Energies 12 (2019) 75.
[31] M. Chereches, A. Vardaru, G. Huminic, E.I. Chereches, A.A. Minea, A. Huminic, Thermal conductivity of stabilized PEG 400 based nanofluids: An experimental approach, Int. Commun. Heat Mass Transf 130 (2022), 105798.
[32] S. Navidbakhsh, R. Majdan-Cegincara, Effect of γ-Fe_2O_3 nanoparticles on rheological and volumetric properties of solutions containing polyethylene glycol, Int. J. Ind. Chem. 8 (2017) 433.
[33] B. Tang, C. Wu, M. Qiu, X. Zhang, S. Zhang, PEG/SiO_2–Al_2O_3 hybrid form-stable phase change materials with enhanced thermal conductivity, Mater. Chem. Phys. 144 (2014) 162.
[34] K. Yapici, N.K. Cakmak, N. Ilhan, Y. Uludag, Rheological characterization of polyethylene glycol based TiO_2 nanofluids, Korea-Aust. Rheol. J. 26 (2014) 355.
[35] J. Sobczak, J.P. Vallejo, J. Traciak, S. Hamze, J. Fal, P. Estellé, L. Lugo, G. Żyła, Thermophysical profile of ethylene glycol based nanofluids containing two types of carbon black nanoparticles with different specific surface areas, J. Mol. Liq. 326 (2021), 115255.
[36] S.U. Ilyas, R. Pendyala, M. Narahari, Stability and thermal analysis of MWCNT-thermal oil-based nanofluids, Colloids Surf A Physicochem Eng Asp 527 (2017) 11.
[37] L. Colla, L. Fedele, S. Mancin, L. Danza, O. Manca, Nano-PCMs for enhanced energy storage and passive cooling applications, Appl. Therm. Eng. 110 (2017) 584.
[38] F. Wang, C. Zhang, J. Liu, X. Fang, Z. Zhang, Highly stable graphite nanoparticle-dispersed phase change emulsions with little supercooling and high thermal conductivity for cold energy storage, Appl. Energy 188 (2017) 97.
[39] C. Lin, Z. Rao, Thermal conductivity enhancement of paraffin by adding boron nitride nanostructures: A molecular dynamics study, Appl. Therm. Eng. 110 (2017) 1411.
[40] N. Trong Tam, N. Viet Phuong, P. Hong Khoi, P. Ngoc Minh, M. Afrand, P. Van Trinh, B. Hung Thang, G. Żyła, P. Estellé, Carbon nanomaterial-based nanofluids for direct thermal solar absorption, Nanomaterials 10 (2020) 1199.
[41] J.P. Vallejo, G. Żyła, L. Ansia, J. Fal, J. Traciak, L. Lugo, Thermophysical, rheological and electrical properties of mono and hybrid TiB_2/B_4C nanofluids based on a propylene glycol:water mixture, Powder Technol. 395 (2022) 391.
[42] J.P. Vallejo, G. Żyła, J. Fernández-Seara, L. Lugo, Influence of six carbon-based nanomaterials on the rheological properties of nanofluids, Nanomaterials 9 (2019) 146.
[43] G. Żyła, Nanofluids containing low fraction of carbon black nanoparticles in ethylene glycol: An experimental study on their rheological properties, J. Mol. Liq. 297 (2020), 111732.
[44] A. Elsaidy, J.P. Vallejo, V. Salgueiriño, L. Lugo, Tuning the thermal properties of aqueous nanofluids by taking advantage of size-customized clusters of iron oxide nanoparticles, J. Mol. Liq. 344 (2021), 117727.
[45] S. Aberoumand, P. Woodfield, G. Shi, T. Kien Nguyen, H.-Q. Nguyen, Q. Li, B. Shabani, D., Viet Dao, Thermo-electro-rheological behaviour of vanadium electrolyte-based electrochemical graphene oxide nanofluid designed for redox flow battery, J. Mol. Liq. 338 (2021), 116860.
[46] S.U. Ilyas, S. Ridha, S. Sardar, P. Estellé, A. Kumar, R. Pendyala, Rheological behavior of stabilized diamond-graphene nanoplatelets hybrid nanosuspensions in mineral oil, J. Mol. Liq. 328 (2021), 115509.
[47] D. Di Rosa, M. Wanic, J. Fal, G. Żyła, L. Mercatelli, E. Sani, Optical and dielectric properties of ethylene glycol-based nanofluids containing nanodiamonds with various purities, Powder Technol. 356 (2019) 508.
[48] ISO 22412 (2017) 2017.
[49] J. Healy, J. De Groot, J. Kestin, The theory of the transient hot-wire method for measuring thermal conductivity, Phys. B+C 82 (1976) 392.
[50] Y. Nagasaka, A. Nagashima, Absolute measurement of the thermal conductivity of electrically conducting liquids by the transient hot-wire method, J. Phys. E Sci. Instrum. 14 (1981) 1435.

[51] M.J. Pastoriza-Gallego, L. Lugo, J.L. Legido, M.M. Piñeiro, Thermal conductivity and viscosity measurements of ethylene glycol-based Al_2O_3 nanofluids, Nanoscale Res. Lett. 6 (2011) 1.
[52] J.P. Vallejo, E. Álvarez-Regueiro, D. Cabaleiro, J. Fernández-Seara, J. Fernández, L. Lugo, Functionalized graphene nanoplatelet nanofluids based on a commercial industrial antifreeze for the thermal performance enhancement of wind turbines, Appl. Therm. Eng. 152 (2019) 113.
[53] D. Cabaleiro, C. Gracia-Fernández, L. Lugo, (Solid+liquid) phase equilibria and heat capacity of (diphenyl ether+biphenyl) mixtures used as thermal energy storage materials, J. Chem. Thermodyn. 74 (2014) 43.
[54] G. Żyła, J. Fal, Experimental studies on viscosity, thermal and electrical conductivity of aluminum nitride–ethylene glycol (AlN–EG) nanofluids, Thermochim Acta 637 (2016) 11.
[55] G. Żyła, J.P. Vallejo, J. Fal, L. Lugo, Nanodiamonds–ethylene glycol nanofluids: experimental investigation of fundamental physical properties, Int. J. Heat Mass Transf. 121 (2018) 1201.
[56] Alpha-A High Resolution Dielectric, Conductivity, Impedance and Gain Phase Modular Measurement System, USER's Manual Issue:9/2010 Rev. 3.1. by Novocontrol Technologies GmbH& Co. KG.
[57] A. Gómez-Merino, J. Jiménez-Galea, F. Rubio-Hernández, J. Arjona-Escudero, I. Santos-Ráez, Heat transfer and rheological behavior of fumed silica nanofluids, Processes 8 (2020) 1535.
[58] K. Dubyk, M. Isaiev, S. Alekseev, R. Burbelo, V. Lysenko, Thermal conductivity of nanofluids formed by carbon flurooxide mesoparticles, SN Appl. Sci 1 (2019) 1.
[59] Q. Sun, Y. Yuan, H. Zhang, X. Cao, L. Sun, Thermal properties of polyethylene glycol/carbon microsphere composite as a novel phase change material, J. Therm. Anal. Calorim. 130 (2017) 1741.
[60] L. Rebrović, A. Jukić, F. Faraguna, Influence of MWCNTs geometry and surface oxidation on rheological and thermal properties of PEG nanofluids, J. Therm. Anal. Calorim. 148 (2023) 1351.
[61] M.E. Spahr, R. Gilardi, D. Bonacchi, Carbon black for electrically conductive polymer applications, Fillers for polymer applications (2017) 375.
[62] D. Lou, T. Grablander, M. Mao, H. Hong, G. Peterson, Improved thermal conductivity of PEG-based fluids using hydrogen bonding and long chain of nanoparticle, J. Nanopart. Res. 23 (2021) 1.
[63] M.A. Marcos, N.E. Podolsky, D. Cabaleiro, L. Lugo, A.O. Zakharov, V.N. Postnov, N. A. Charykov, S.V. Ageev, K.N. Semenov, MWCNT in PEG-400 nanofluids for thermal applications: A chemical, physical and thermal approach, J. Mol. Liq. 294 (2019), 111616.
[64] Z. Liu, H. Wei, B. Tang, S. Xu, Z. Shufen, Novel light–driven CF/PEG/SiO_2 composite phase change materials with high thermal conductivity, Sol. Energy Mater. Sol. Cells 174 (2018) 538.
[65] M.A. Marcos, D. Cabaleiro, M.J. Guimarey, M.J. Comuñas, L. Fedele, J. Fernández, L. Lugo, PEG 400-based phase change materials nano-enhanced with functionalized graphene nanoplatelets, Nanomaterials 8 (2018) 16.
[66] J. Yang, L.-S. Tang, R.-Y. Bao, L. Bai, Z.-Y. Liu, W. Yang, B.-H. Xie, M.-B. Yang, Largely enhanced thermal conductivity of poly (ethylene glycol)/boron nitride composite phase change materials for solar-thermal-electric energy conversion and storage with very low content of graphene nanoplatelets, Chem. Eng. J. 315 (2017) 481.
[67] Z. Mingzheng, X. Guodong, L. Jian, C. Lei, Z. Lijun, Analysis of factors influencing thermal conductivity and viscosity in different kinds of surfactant solutions, Exp. Therm Fluid Sci. 36 (2012) 22.
[68] R. Francesconi, A. Bigi, K. Rubini, F. Comelli, Molar heat capacities, densities, viscosities, and refractive indices of poly (ethylene glycols)+ 2-methyltetrahydrofuran at (293.15, 303.15, and 313.15) K, J. Chem. Eng. Data 52 (2007) 2020.
[69] N.E. Podolsky, M.A. Marcos, D. Cabaleiro, K.N. Semenov, L. Lugo, A.V. Petrov, N. A. Charykov, V.V. Sharoyko, T.D. Vlasov, I.V. Murin, Physico-chemical properties of C60(OH)22–24 water solutions: density, viscosity, refraction index, isobaric heat capacity and antioxidant activity, J. Mol. Liq. 278 (2019) 342.
[70] S. Ottani, D. Vitalini, F. Comelli, C. Castellari, Densities, viscosities, and refractive indices of poly (ethylene glycol) 200 and 400+ cyclic ethers at 303.15 K, J. Chem. Eng. Data 47 (2002) 1197.
[71] J.M. Vuksanović, E.M. Živković, I.R. Radović, B.D. Djordjević, S.P. Šerbanović, M. L. Kijevčanin, Experimental study and modelling of volumetric properties, viscosities and refractive indices of binary liquid mixtures benzene+ PEG 200/PEG 400 and toluene+ PEG 200/PEG 400, Fluid Phase Equilib. 345 (2013) 28.
[72] T.Y. Wu, H.C. Wang, S.G. Su, S.T. Gung, M.W. Lin, C.B. Lin, Characterization of ionic conductivity, viscosity, density, and self-diffusion coefficient for binary mixtures of polyethyleneglycol (or polyethyleneimine) organic solvent with room temperature ionic liquid BMIBF4 (or BMIPF6), J. Taiwan Inst. Chem. Eng. 41 (2010) 315.
[73] N. Živković, S. Šerbanović, M. Kijevčanin, E. Živković, Volumetric properties, viscosities, and refractive indices of the binary systems 1-butanol+ PEG 200,+ PEG 400, and+ TEGDME, Int. J. Thermophys. 34 (2013) 1002.
[74] L. Zhang, H. Sun, B. Han, L. Peng, F. Ning, G. Jiang, V. Chehotkin, Effect of shearing actions on the rheological properties and mesostructures of CMC, PVP and CMC+PVP aqueous solutions as simple water-based drilling fluids for gas hydrate drilling, J. Unconv. Oil Gas Resour. 14 (2016) 86.
[75] R.J. Sengwa, S. Choudhary, P. Dhatarwal, Effect of ionic contaminants on dielectric dispersion and relaxation processes over static permittivity frequency region in neat liquid poly(ethylene glycol), J. Mol. Liq. 220 (2016) 1042.
[76] R. Sengwa, S. Choudhary, S. Sankhla, Low frequency dielectric relaxation processes and ionic conductivity of montmorillonite clay nanoparticles colloidal suspension in poly (vinyl pyrrolidone)-ethylene glycol blends, Express Polym Lett 2 (2008) 800.
[77] R. Sengwa, S. Sankhla, Dielectric dispersion study of poly (vinyl pyrrolidone)–polar solvent solutions in the frequency range 20 Hz–1 MHz, J. Macromol. Sci. Part B Phys. 46 (2007) 717.
[78] M. Saraswat, R.J. Sengwa, Investigation on ethylene glycol and glycerol mixture concentration dependent optical, dielectric, electrical, rheological, and thermophysical properties of EG+Gly/ZnO semiconductor nanofluids, Phys. E Low Dimens. Syst. Nanostruct. 150 (2023), 115700.